Abdominal Radiology (2021) 46:2540–2555
https://doi.org/10.1007/s00261-020-02924-6

REVIEW

Imaging of calcified hepatic lesions: spectrum of diseases

Giuseppe Mamone[1] · Ambra Di Piazza[1] · Giovanni Gentile[1] · Mariapina Milazzo[1] · Vincenzo Carollo[1] · Francesca Crinò[1] · Gianluca Marrone[1] · Settimo Caruso[1] · Gianvincenzo Sparacia[1] · Luigi Maruzzelli[1] · Roberto Miraglia[1]

Received: 23 October 2020 / Revised: 13 December 2020 / Accepted: 19 December 2020 / Published online: 16 January 2021

Abstract
Hepatic calcifications have been increasingly identified over the past decade due to the widespread use of high-resolution Computed Tomography (CT) imaging. Calcifications can be seen in a vast spectrum of common and uncommon diseases, from benign to malignant, including cystic lesions, solid neoplastic masses, and inflammatory focal lesions. The purpose of this paper is to present an updated review of CT imaging findings of a wide range of calcified hepatic focal lesions, which can help radiologists to narrow the differential diagnosis.

Keywords Calcified hepatic lesion · Liver calcification · Computed tomography (CT) · Differential diagnosis

Introduction

Hepatic calcifications can be seen in a wide variety of disorders, including cystic lesions, benign and malignant solid neoplastic masses, and inflammatory focal lesions [1, 2].

However, the most common causes are hydatidosis, granulomatous diseases, and neoplastic lesions. Indeed, it is believed that the small round or amorphous calcifications often encountered in the liver during a CT scan are likely aspecific granuloma (Fig. 1).

Because of its high contrast and spatial resolution with very thin slice acquisition, CT is the best and most sensitive imaging technique to detect and to evaluate hepatic calcifications. Knowledge of the CT imaging findings of focal liver focal lesions associated with calcifications is central to improving the diagnostic accuracy. However, only a few reviews of this topic are available in the literature [1, 2]. Our purpose is to familiarize radiologists with the wide range of common and uncommon hepatic lesions associated with calcifications. Vascular and biliary causes of hepatic calcifications, such as hepatic artery aneurysm, intrahepatic portal vein thrombosis, portal hypertension, traumatic lesions, and intrahepatic biliary stones will not be discussed because they are not associated with focal lesions.

Calcifications and hepatic lesions

Calcifications in hepatic lesions can occur in different patterns, which can be solitary or multiple. According to the location inside the lesion, calcifications may be mural (such as in cystic lesions), peripheral, or central. The morphology of these calcifications ranges from linear to punctate, nodular, or amorphous. Regarding their origins, they are caused by hemorrhage, necrosis, inflammation, or are related to the histopathology of the lesion.

Cystic hepatic lesions associated with calcifications include simple cyst, mucinous cystic neoplasm, hydatidosis, polycystic liver disease, and Caroli disease.

Hepatic hemangioma and adenoma are benign lesions which can show internal calcifications. The most common solid primary malignant lesions of the liver showing intralesional calcifications are fibrolamellar carcinoma, hepatoblastoma, intrahepatic cholangiocarcinoma, and epithelioid hemangioendothelioma. In hepatocellular carcinoma (HCC), the presence of calcifications is rare. Furthermore, intralesional calcifications may be present in other uncommon malignant hepatic lesions, such as primary neuroendocrine tumor, sarcoma, PEComa, and solitary fibrous tumor.

✉ Giuseppe Mamone
gmamone@ismett.edu

[1] Radiology Unit, Department of Diagnostic and Therapeutic Services, IRCCS ISMETT (Mediterranean Institute for Transplantation and Advanced Specialized Therapies), via Tricomi 5, 90127 Palermo, Italy

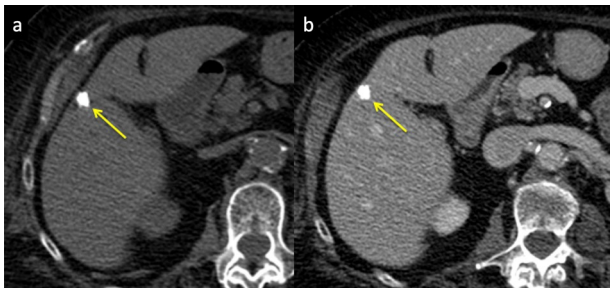

Fig. 1 Granuloma. Unenhanced CT image (**a**) and portal phase contrast-enhanced CT image (**b**) show a small mildly lobulated calcification in the right hepatic lobe (arrows), usually related to an aspecific granuloma

Inflammatory diseases are the most common cause of calcified hepatic lesions in the liver parenchyma, and include infections, and rarely sarcoidosis [1, 2]. Furthermore, inflammatory disorders characterized by granulomatous lesions are the most common cause of hepatic calcification. A wide range of infections can causes hepatic calcification, including

- *Viral infection*: cytomegalovirus
- *Bacterial infection*: chronic pyogenic abscess (e.g., from E. Coli, K. Pneumoniae, Streptococcus), tuberculosis, brucellosis, syphilitic gumma
- *Fungal infection*: histoplasmosis, coccidioidomycosis, Pneumocystis jirovecii
- *Parasitic infection*: hydatid disease, chronic amebic abscess from Entamoeba histolytica, toxoplasmosis, schistosomiasis, fascioliasis, cysticercosis, filariasis, paragonimiasis, dracunculiasis, Armillifer infection.

Since it is known that the morphologic appearances of calcifications alone do not allow a specific diagnosis, the association with other imaging findings of the calcified lesions, such as the dynamic contrast-enhanced pattern, may indicate the correct diagnosis or narrow the differential diagnosis. Therefore, we decided to provide a new approach according to the dynamic contrast-enhanced pattern of calcified hepatic focal lesions (Fig. 2, Table 1), instead of a classification based on the calcifications pattern.

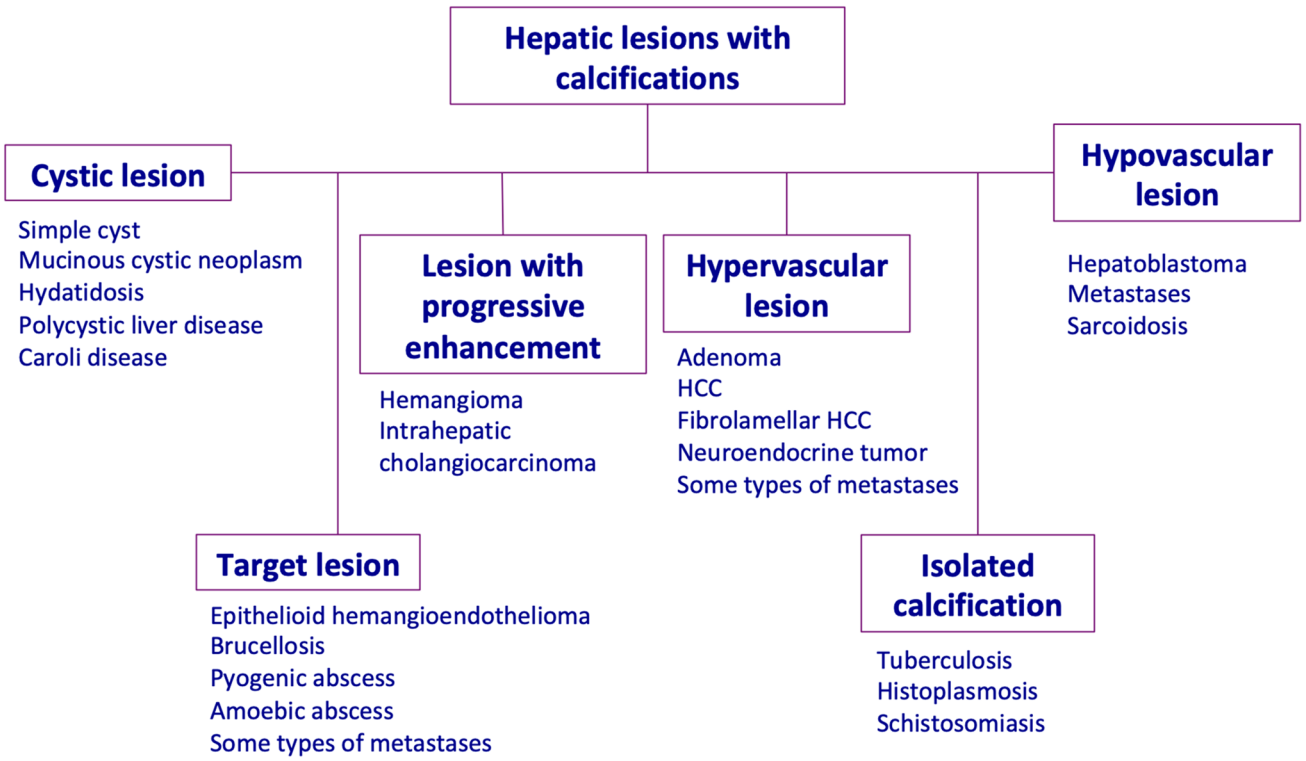

Fig. 2 Illustration of a diagnostic approach to calcified hepatic lesions according to the dynamic contrast-enhanced pattern

Table 1 Diagnostic approach to hepatic calcified lesions

Contrast-enhanced pattern	Hepatic lesion	Pattern of calcifications	Other common findings
Cystic appearance	Simple cyst	Wall calcifications (rare)	Well-defined lesions with smooth imperceptible walls, serous fluid, and absence of internal nodularity, mural irregularity, or septation
	Mucinous cystic neoplasm	Septal and mural calcifications (25–27%)	Large, multiloculated, well-circumscribed cystic masses with a wall, inner septa, and nodules that enhance
	Hydatidosis	Wall calcifications (type II) totally calcified (type Ill)	Unilocular or multilocular cystic lesion according to the four radiologic patterns
	Polycystic liver disease	Cystic wall partial or totally calcified	Enlarged liver with multiple thin-walled cysts of varying size, with simple fluid or increased attenuation in case of hemorrhage or infection
	Caroli disease	Punctate calcifications	Saccular or fusiform cystic dilatations of the intrahepatic bile ducts up to 5 cm in diameter, often containing calculi or sludge, central dot sign
Lesions with progressive enhancement	Cavernous emangioma	Coarse and central calcifications	Peripheral globular enhancement (puddling; it follows the enhancement of the aorta) followed by a slow, progressive, and centripetal filling; or sclerosing/sclerosed hemangioma pattern
	Intrahepatic cholangiocarcinoma	Solitary or multiple, amorphous, and central calcifications (18%)	Peripheral enhancement in arterial phase followed by progressive centripetal enhancement in late phases
Hypervascular lesions	Adenoma	Solitary or multiple, discrete and heterogeneous, and central or eccentric (5–10%); associated with areas of old hemorrhage or necrosis	Imaging features reflect the tumor subtypes
	HCC	Curvilinear, scattered punctate, or globular pattern (7.5–9%)	Arterial enhancement followed by wash-out with capsular enhancement on portal venous and/or delayed phase images
	Fibrolamellar HCC	Punctate, nodular, or stellate calcifications (67–68%), often involving the central scar	Large lobulated mass with central scar, complete or incomplete tumor pseudocapsule, enhancement on arterial phase with or without wash-out during portal and delayed phases; lymph node metastasis
	Neuroendocrine tumor	Coarse, central, or peripheral calcifications (rare)	Hypervascular during the arterial phase; wash-out is present on delayed phases in 48% of cases; internal necrosis or hemorrhage
Hypovascular lesions	Hepatoblastoma	Amorphous and coarse but also punctate, speckled, or curvilinear calcifications (20–50%)	Large multilobulated mass with heterogeneous enhancement to a lesser degree than the surrounding liver parenchyma in both arterial and portal venous/delayed phases; children < 5 years of age
	Metastases	Amorphous, stippled, sand-like or granular calcifications, central or peripheral in location (11% of cases in colorectal ca, 5% after chemotherapy)	Hypodense multiple lesions
	Sarcoidosis	Pattern of calcifications not clearly described; rare but can be seen in long-standing disease	Hepatosplenomegaly, diffuse hepatic and splenic parenchymal heterogeneity or multiple hypodense small lesions scattered throughout the liver(< 2 cm); other organs involved (lung)

Table 1 (continued)

Contrast-enhanced pattern	Hepatic lesion	Pattern of calcifications	Other common findings
Lesions with target appearance	Epithelioid hemangioendothelioma	Coarse, dystrophic, and central calcifications (in up to 20%)	Multiple, peripheral, coalescent lesions with target-like appearance (2 or 3 layers); capsular retraction; lollipop sign
	Brucellosis	Central solitary calcification, surrounded or not by a fluid collection	Heterogeneously hypodense lesions; a peripheral enhancing rim may even be seen
	Pyogenic abscess	Central or peripheral calcifications in chronic abscesses or in some residual lesions	Different patterns: hypoattenuating lesions with peripheral enhancement; lesion with the "double target sign"; lesion with the "cluster sign"
	Amoebic abscess	Peripheral calcifications in chronic abscesses or after healing	Usually unilocular and located near the hepatic capsule, with a complex fluid attenuation in the central part of the lesion and a capsule with rim enhancement, or the "double target sign"
Isolated calcifications	Tuberculosis	Solitary or multiple, calcification typically involving the entire lesion in clinically occult or healed lesions	The miliary type is the most common pattern: numerous, small (< 2 cm), and hypodense nodules scattered throughout the liver; calcified lesions in the spleen and lungs
	Histoplasmosis	Multiple small calcification typically involving the entire lesion in healed disease	Multiple, small (< 2 cm), and hypodense nodules scattered throughout the liver; calcified lesions in the spleen and lungs
	Schistosomiasis	Capsular and peripheral septal calcifications; "turtle back" pattern	Multiple peripheral subcapsular and periportal wedge-shaped hypoattenuating regions associated with capsular retraction

Fig. 3 Simple cyst. Unenhanced CT image (**a**) and portal phase contrast-enhanced CT image (**b**) exhibit a large simple cyst in the right hepatic lobe, showing a punctate calcification along its thin wall (arrows)

Calcifications in cystic lesions

Simple cyst

Simple hepatic cysts are common benign cysts, representing about 60% of focal hepatic lesions and occurring in 2.5% of the general population [3].

They refer to benign developmental cysts of biliary origin as a result of deranged development of the biliary tree. They vary in size and can be solitary or multiple, without communication with the biliary system. Simple cysts appear as well-defined lesions with smooth imperceptible walls, serous fluid, and absence of internal nodularity, mural irregularity, or septation. On CT, simple cysts are typically well-circumscribed homogeneously hypodense lesions, with water density and absence of both enhancing nodules and wall enhancement [3, 4]. Cyst wall calcifications are uncommon and usually related to complications, such as hemorrhage or superinfection, where the development of internal septations and increased or heterogeneous attenuation may be present (Fig. 3) [3].

Mucinous cystic neoplasm (biliary cystadenoma/cystadenocarcinoma)

Mucinous cystic neoplasms (MCNs), previously called biliary cystadenomas and cystadenocarcinomas, are uncommon cystic tumors arising from the intrahepatic biliary duct system in 85% of cases, and from the extrahepatic ducts or gallbladder in the remaining 15% [4, 5]. The WHO has classified them as “mucinous cystic neoplasm with low-, intermediate-, or high-grade intraepithelial neoplasia” and “mucinous cystic neoplasm with invasive carcinoma” (malignant mucinous cystic neoplasm), rather than the previous terms “biliary cystadenoma” and “biliary cystadenocarcinoma” [6]. Hepatic MCNs represent less than 5% of all the hepatic cystic lesions, and are more common in middle-aged women. They vary in size, ranging from small

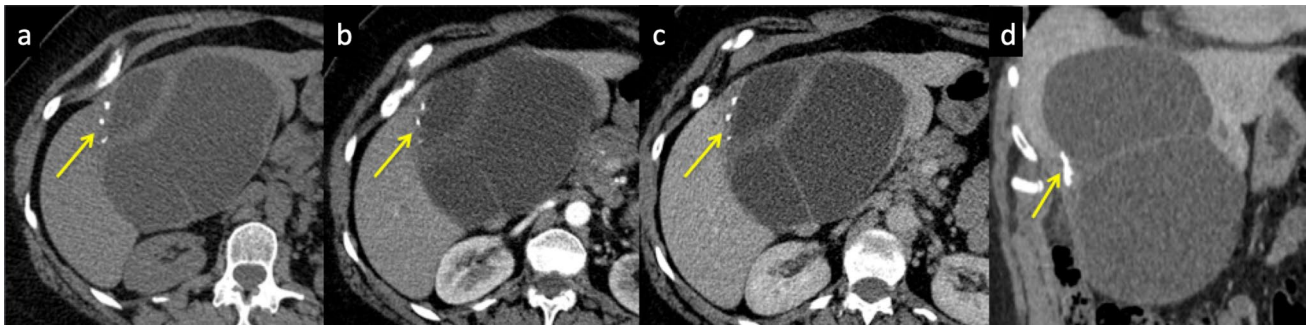

Fig. 4 Mucinous cystic neoplasm. Unenhanced (**a**) and contrast-enhanced CT axial images on arterial (**b**) and portal venous (**c**) phases exhibit a large and well-circumscribed cystic lesion with wall and inner septa, showing small mural calcifications (arrows). These calcifications are visualized also on coronal plane reconstruction (arrow) (**d**)

to large lesion (up to 35 cm) [2], and appear hypoattenuating on unenhanced CT images. After contrast agent administration, MCNs usually appear as large, multiloculated, well-circumscribed cystic masses with a wall, inner septa, and nodules that enhance [4, 5]. Enhancing nodules larger than 1 cm indicate high risk of malignancy. MCNs are not connected to the biliary system. Septal and mural calcifications can be present, and have been reported in 25–27% of cases in small series (Fig. 4) [7, 8]. The best treatment option for MCNs is hepatic resection.

Hydatidosis

Liver hydatidosis is a zoonosis caused by infestation with Echinococcus tapeworm, and is endemic in many parts of the world. There are two types of Echinococcus infections: cystic hydatidosis due to Echinococcus granulosis, and alveolar hydatidosis due to Echinococcus multilocularis. The former is the more common type, and presents as a cystic lesion. By contrast, alveolar hydatidosis is less common, and shows an infiltrative appearance that can mimic a malignancy. It presents as an infiltrative hypodense ill-defined lesions on CT, with areas of necrosis resulting in central irregular calcifications in 90% of patients infected [2]. The liver is the most commonly organ affected (60–75% of cases), with 80% of hydatid cysts located in the right lobe. The WHO 2001 classification, as a review of the Gharbi classification of 1981, provides a standardized approach for the diagnosis of hydatid cyst on ultrasound. On CT, the hydatid cyst appears as a unilocular or multilocular cystic lesion according to the four radiologic patterns described [9, 10].

Type I: simple well-defined cyst with fluid attenuation density and absence of internal contents. It may be difficult to distinguish this type from simple epithelial cyst; the presence of enhancing cystic wall, representing the pericyst, is a finding that helps to differentiate type I from a simple liver cyst.

Type II (a, b, c): cyst with daughter cysts and matrix. Floating membranes can also be seen in the cyst. Daughter cysts are visible as round or oval structures located within the mother cyst, typically arranged at the periphery (type IIa). They usually contain fluid with a lower attenuation than that of the fluid of the mother cyst. Larger, irregularly shaped daughter cysts can occupy almost the entire volume of the mother cyst (type IIb). Scattered, peripheral calcification may occur along the wall and is easily detected in CT images as a curvilinear or ring-like structure (type IIc).

Type III: non-viable cyst totally calcified.

Type IV: hydatid cyst complications, including infection and rupture caused by degeneration of hydatid membranes (contained, communicating, or direct). CT images may depict gas or air-fluid levels or fat within the hydatid cyst as an indirect signs of infection or communication with the biliary system. However, the presence of fat can be related to degeneration of hydatid membranes due to the aging process of the cyst.

Therefore, partial calcification of the cyst wall does not indicate the death of the parasite, while heavily calcified cysts can be assumed to be inactive (Fig. 5) [9].

These calcifications are easily detected on CT, which also represents an important diagnostic tool for recognizing complications, such as rupture and infections, and therefore for assessing resectability.

Polycystic liver disease

Polycystic liver diseases (PLD) include a spectrum of genetic disorders characterized by cholangiocyte-derived fluid-filled cysts that gradually replace liver tissue. PLD occurs in combination with autosomal dominant polycystic kidney disease (ADPKD) and autosomal recessive polycystic kidney disease (ARPKD), as well as alone (autosomal dominant PLD: ADPLD) [11]. ADPKD is the most common inherited nephropathy since approximately half of ARPKD neonates

Fig. 5 Hydatidosis. Unenhanced (**a**) and dynamic contrast-enhanced CT axial images on arterial (**b**), portal venous (**c**), and delayed (**d**) phases show a large lobulated cystic lesion with coarse calcifications in the wall and internal contents. This totally calcified lesion is a non-viable hydatid cyst (Type III)

die shortly after birth due to pulmonary hypoplasia. Hepatic involvement occurs in 30–70% of patients with ADPKD, where the development of hepatic cysts lags behind the onset of renal cysts, and the number and size of cysts increase with advancing age [11]. ADPLD is much less common and milder than ADPKD, and it is characterized by the presence of cysts mainly in the liver with no or very few renal cysts, with disease progression into adulthood. In patients with PLD, intrahepatic cysts and peribiliary cysts are present, which do not communicate with the biliary system but can occasionally cause biliary obstruction or cholangitis.

Intrahepatic cysts are more common and mostly peripheral, while peribiliary cysts are typically less than 10 mm in size, appearing as a string of cysts or tubular structures along the portal vessels, from the perihilar area to the third-order bile duct branches [11].

On CT imaging, these patients typically show an enlarged liver, with multiple thin-walled cysts of varying size (from 1 mm to 12 cm), with low attenuation of simple fluid; however, cysts complicated by hemorrhage or infection may be seen as increased attenuation on CT and fluid–fluid levels may also be present [11]. On contrast-enhanced CT images, the cysts show smooth walls, and usually septations or enhancing mural nodules are absent [11]. The cystic wall may appear partial or totally calcified (Fig. 6), usually as a result of previous hemorrhage and inflammation. Despite impressive radiologic findings, only a minority of patients with PLD will progress to end-stage liver disease or develop complications such as infection, compression of biliary system, bleeding, or rupture of the cysts. The differential diagnosis includes multiple simple cysts, biliary hamartoma, Caroli disease, and hydatid cysts. In PLD, the cysts are typically innumerable (more than 20 cysts) and of varying sizes, with replacement of over 50% of the liver; furthermore, cysts can be seen in the kidneys.

Caroli disease

Caroli disease (CD) is a fibropolycystic disease characterized by multifocal segmental dilatation of the large intrahepatic bile ducts, which retain their communication with the biliary tree [11]. There are two types of CD: Caroli disease proper or so-called "pure" form, and the more common Caroli syndrome, in which the bile duct dilatation is less

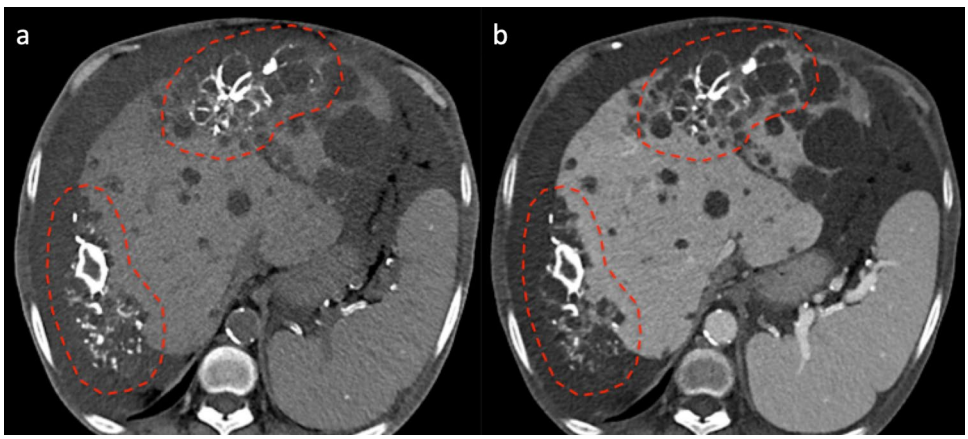

Fig. 6 Polycystic liver disease. Unenhanced CT image (**a**) and portal phase contrast-enhanced CT image (**b**) show an enlarged liver with multiple cysts, mostly peripheral, some of them appear partially or totally calcified (red lines)

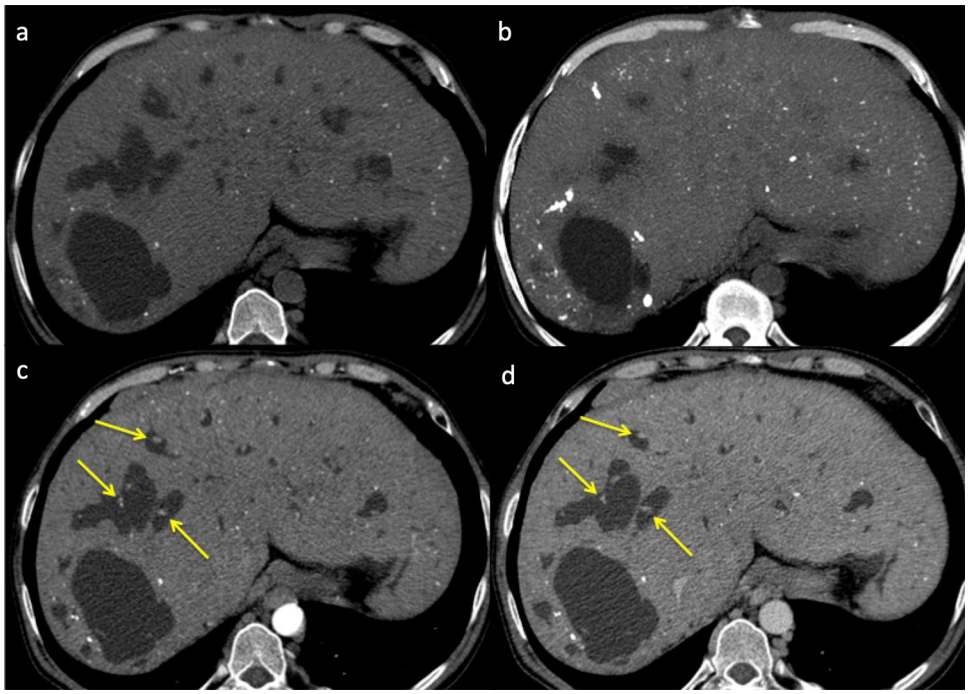

Fig. 7 Caroli disease. Unenhanced CT image (**a**) shows multiple punctate calcifications of the liver, associated with cystic hypodense lesions represented by saccular and fusiform dilatations of the intrahepatic bile ducts. These calcifications are better visualized on MIP reconstruction of unenhanced CT image (**b**). On arterial (**c**) and portal venous (**d**) contrast-enhanced CT imaging, notice the presence of "central dot sign" (arrows), a finding highly suggestive of Caroli disease that consists of enhancing fibrovascular bundles within the biliary dilatations

marked and a variable degree of congenital hepatic fibrosis or other fibropolycystic liver diseases are present. Imaging findings of CD typically are saccular or fusiform cystic dilatations of the intrahepatic bile ducts up to 5 cm in diameter, often containing calculi or sludge, associated with punctate calcifications (Fig. 7) [11]. A finding highly suggestive of CD is the "central dot sign," which consists of enhancing fibrovascular bundles within the biliary dilatations. It corresponds to a small portal vein branch and an accompanying hepatic artery branch protruding into the lumen of a dilated bile duct [11]. The clinical signs of CD are produced by bile stasis. The latter leads to development of stones favoring infections, cholangitis, liver abscesses, and secondary biliary cirrhosis if chronic biliary obstruction occurs. Furthermore, a prevalence of 7% of cholangiocarcinoma in these patients has been reported. The main differential diagnosis includes polycystic liver disease, primary sclerosing cholangitis (PSC), and clonorchiasis.

Calcifications in lesions with progressive enhancement

Hemangioma

The hemangioma is the most common solid lesion of the liver, with an incidence of up to 20% [12]. This benign lesion is often found incidentally at any age, and is more frequent in females (F/M ratio of 2–5:1). Currently, hepatic hemangioma is known as a slow flow venous malformation according to the newest classification system of the International Society for the Study of Vascular Anomalies (ISSVA), last updated in 2018 (http://www.issva.org/UserFiles/file/ISSVA--Classification-2018.pdf).

Hemangiomas are vascular lesions with round or lobulated shape and well-defined margins. They are unique or multiple (10–50% of cases) and more commonly seen at periphery of the liver; however, they can occur anywhere in the hepatic parenchyma, in particular along the hepatic veins [12]. Since their size varies from a few millimeters to more than 20 cm, they are classified as small (< 1.5 cm), medium (1.5–5 cm), and large HH (> 5 cm). Regarding the two typical forms of hemangioma, cavernous hemangioma (CH), and flash-filling hemangioma, it is the former that may rarely show calcifications.

CH appears hypodense, similarly to the liver vessels on unenhanced CT, and shows a typical pattern after contrast agent administration, represented by a peripheral globular discontinuous enhancement (puddling) followed by a slow, progressive, and centripetal filling [12]. This progressive filling is explained by the slow blood flow within its vascular spaces, follows the enhancement of the aorta, and can be complete or incomplete. An incomplete contrast filling is usually observed in large or giant lesions, due to the presence of thrombohemorrhagic component, fibrosis, hyalinization, or cystic degeneration. In these lesions, calcifications are rare and have been reported in 10% of the ultrasound images and 20% of CT scans [1, 12, 13]. They are frequently coarse and located in areas of central fibrosis, but can also be peripheral and punctate (Fig. 8) [2]. Calcified hemangiomas

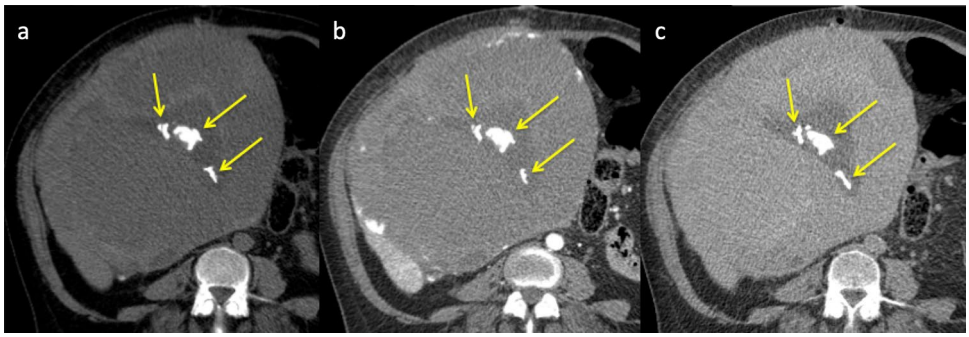

Fig. 8 Hemangioma. Unenhanced (**a**) and contrast-enhanced CT axial images on arterial (**b**) and 10 min delayed (**c**) phases, exhibit a giant hemangioma with the typical pattern represented by a peripheral globular discontinuous enhancement (puddling) followed by a slow, progressive, and centripetal filling. This lesion shows a central hypodense area, usually related to thrombohemorrhagic component, fibrosis, hyalinization or cystic degeneration, associated with multiple, coarse, and amorphous calcifications (arrows)

can exhibit the above-mentioned typical enhancement in contrast-enhanced CT or a poor enhancement as a sclerosed/sclerosing hemangioma [12].

Intrahepatic cholangiocarcinoma

Intrahepatic cholangiocarcinoma (ICC) is the second most common primary malignancy of the liver (10–20%) [6]. Risk factors include primary sclerosing cholangitis, fibropolycystic liver disease, chronic intrahepatic stone disease, cirrhosis, parasitic infection, and toxins.

ICC arises from biliary cells and can show three growth patterns: mass-forming, periductal infiltrating, and intraductal [6, 14]. The mass-forming type is the most common, with lobulated and often well-defined margins. On CT imaging, the typical enhancement pattern of ICC is characterized by peripheral enhancement in arterial phase followed by progressive centripetal enhancement in late phases, reflecting the presence of vascularized cells located at the periphery and internal desmoplasia [6, 14]. On unenhanced CT, ICC appears as a hypoattenuating mass, and calcifications have been reported in 18% of cases, often associated with desmoplastic reaction in the central part of the lesion (Fig. 9), which can be solitary or multiple with ill-defined morphology [2].

Other imaging findings include biliary ductal dilatation, satellite nodules, and capsular retraction, reflecting the fibrotic component of the ICC [6, 14]. Differently from HCC, vascular infiltration is a rare finding.

Calcifications in hypervascular lesions

Adenoma

Hepatocellular adenomas (HCAs) are uncommon benign liver neoplasms with malignant potential that typically affect young women using oral contraceptives, but also men using anabolic steroids. Additional risk factors have been reported,

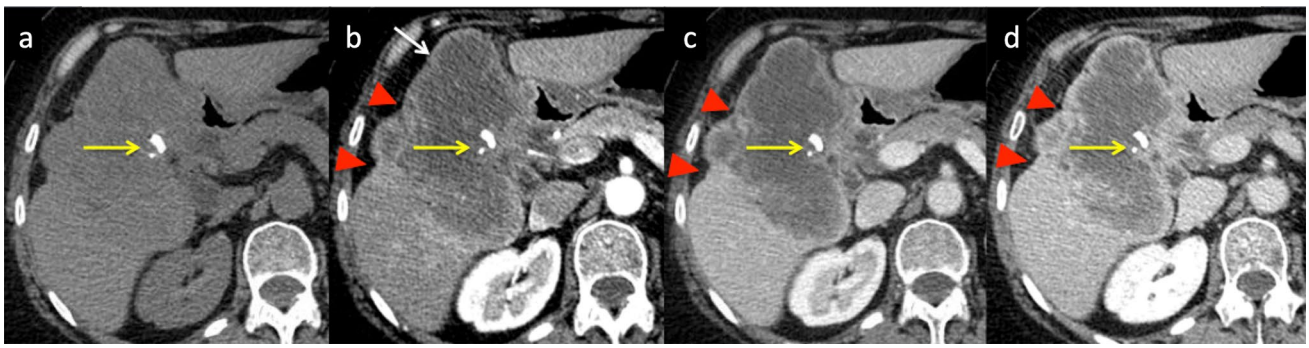

Fig. 9 Intrahepatic cholangiocarcinoma. Unenhanced (**a**) and dynamic contrast-enhanced (**b**–**d**) CT images show a large lobulated hepatic lesion, characterized by rim enhancement on arterial phase (white arrow) followed by progressive incomplete filling on delayed phase (**d**) and capsular retraction (red arrowheads). This typical pattern of mass-forming cholangiocarcinoma is associated with eccentric calcifications (yellow arrows), often associated with desmoplastic reaction

including glycogenosis type 1A, obesity, alcohol, vascular liver disease, and familial adenomatous polyposis.

A molecular classification by Nault et al. [15] has divided HCAs into several subgroups linked with risk factors, clinical behavior, histological features, and imaging:

HNF1 α-inactivated HCA, Inflammatory HCA, CTNNB1 (catenin β1)-mutated HCA in exon 3, CTNNB1 (catenin β1)-mutated HCA in exon 7 and 8, sonic hedgehog HCA, and unclassified HCA. HCAs are associated with complications such as bleeding (15–20% of cases) or malignant transformation into hepatocellular carcinoma (5% of cases treated by liver resection) [15]. Male gender, presence of CTNNB1 (catenin β1)-mutated HCA in exon 3, and size > 5 cm are associated with a high risk of malignant transformation (10%), while the sonic hedgehog HCA, the inflammatory HCA, and a size > 5 cm are associated with a risk of bleeding. HCAs present as a solitary lesion ranging in size from 1 to 30 cm or as multiple lesions. The presence of more than ten HCAs in the liver is defined as "liver adenomatosis."

The imaging features of HCA reflect the tumor subtypes; though CT imaging may suggest some subtypes, MR imaging is the much more accurate diagnostic technique.

HCAs present as hypervascular lesions on the arterial phase; this arterial enhancement is strong in inflammatory HCA, the most common subtype, followed by HNF1α HCA [16].

The wash-out on portal and/or delayed phase CT images is usually shown by HNF1α HCA, while inflammatory HCA shows often persistent enhancement on delayed phase, mimicking an FNH [16]. The presence of diffuse fat within the lesion is the hallmark feature of HNF1α HCA, characterized by diffuse hypodensity with negative density values on unenhanced CT images; to note, this represents a favorable prognostic finding, indicating lack of β-catenin activation [16]. The CT imaging features of the other subtypes of HCA are not specific, and it can be difficult to differentiate these neoplasms from HCC or, rarely, FNH. Indeed, when an HCA shows wash-out on delayed phase images, a capsule appearance is often associated. Liver steatosis can be found in all HCA subgroups; in particular, it is usually associated with inflammatory HCA and may be observed in some HNF1 α inactivated HCAs, and in sonic hedgehog HCA as well [16, 17]. HCAs with acute or chronic hemorrhage, in particular sonic hedgehog HCAs, present as heterogeneous lesions on CT imaging. Calcifications are observed in only 5–10% of HCAs, and are often discrete and heterogeneous, associated with areas of old hemorrhage or necrosis, central or eccentric in location, and solitary or multiple [18, 19].

Hepatocellular carcinoma (HCC)

HCC is the most common primary hepatic malignancy, arising in both liver cirrhosis (80%) and non-cirrhotic liver (20%). Other than cirrhosis, further causes that can induce the development of HCC include HBV viral hepatitis, exposure to Aflatoxin B1, inherited diseases (hemochromatosis, alpha-1 antitrypsin deficiency, type I glycogen storage disease, porphyria), metabolic syndrome, and non-alcoholic fatty liver disease, including non-alcoholic steatohepatitis (NASH), use of anabolic steroids, and degeneration of hepatocellular adenoma.

HCC usually appears as a single mass, though a multifocal or infiltrative pattern may be present. On contrast-enhanced CT imaging, HCC shows a typical pattern characterized by arterial enhancement followed by wash-out with capsular enhancement on portal venous and/or delayed phase images [6]. In HCC arising in patients with cirrhosis, chronic hepatitis B infection, or in patients with previous HCC, the use of the Liver Imaging Reporting and Data System (LI-RADS) algorithm is recommended to provide standardized terminology, techniques, interpretations, and reporting [20].

Vascular invasion, more commonly involving the portal vein than the hepatic veins, and peripheral satellite lesions

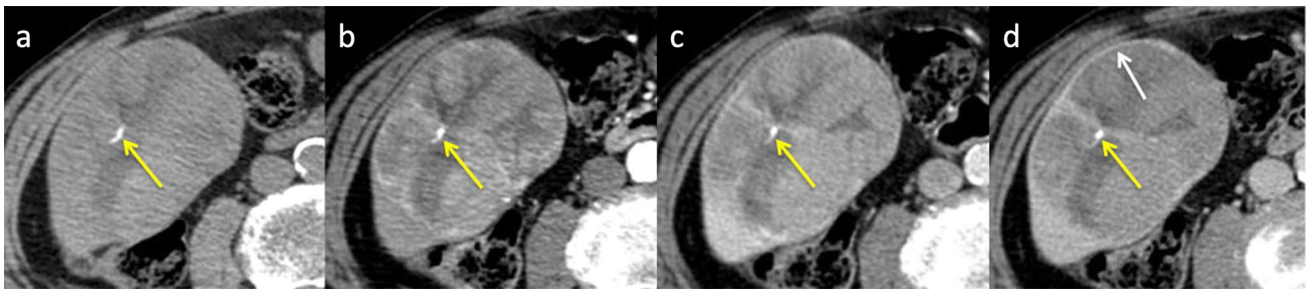

Fig. 10 Hepatocellular carcinoma (HCC). Unenhanced (**a**) and dynamic contrast-enhanced (**b**–**d**) CT images show a large well-defined hypervascular hepatic lesion (**b**) with internal necrotic areas and characterized by wash-out and pseudocapsule (white arrow) on the delayed phase (**d**). Notice the presence of a solitary small calcification in the central part of the lesion (yellow arrows)

may be present. HCC can also show intralesional hemorrhagic areas and necrosis, while the presence of calcifications is rare (Fig. 10). Indeed, calcifications have been reported in 7.5% of HCC by Freeny et al. [21] and in 9% of cases by Stevens et al. [22], though they are more commonly associated with fibrolamellar carcinoma. In these studies, calcifications showed a curvilinear, scattered punctate, or globular pattern.

Fibrolamellar HCC

Fibrolamellar variant of non-cirrhotic HCC is an uncommon form (5%) that arises in young patients (2nd and 3rd decades of life) with a healthy liver [6]. This tumor is more prevalent in Europe and North America, and has a better prognosis than conventional HCC. Tumor markers such as serum α-fetoprotein levels are normally not elevated.

Fibrolamellar HCC (FHCC) appears as a large solitary mass, with well-defined and lobulated margins [6]; a complete or incomplete tumor pseudocapsule has been reported in 30–35% of tumors. On dynamic contrast-enhanced CT imaging, these lesions show inhomogeneous enhancement on arterial phase with or without wash-out during portal and delayed phases [6]. A central scar is often detected inside the lesion (71–73% of cases), with radial septa and stellate shape [23, 24], and usually hypoattenuating during arterial and portal venous phases [6].

Differently from conventional HCC, calcifications can be found in 67–68% of FHCC, often involving the central scar (Fig. 11) [6], and may be punctate, nodular, or stellate. These calcifications help in the differential diagnosis, including FNH, hepatic adenoma, and conventional HCC, where calcifications are rarely reported.

Furthermore, large areas of hemorrhage are uncommon, and fat is usually absent [6]. Importantly, lymph node metastasis is reported in 65% of FHCCs and peritoneal carcinosis is not rare at the time of diagnosis [6]. Vascular invasion has also been described [6], and distant metastases occur in approximately 20–30% of cases, in particular in adrenal glands and lung [2].

Neuroendocrine neoplasm

Primary neuroendocrine neoplasm (NEN) of the liver is an extremely rare tumor (0.3% of all NENs) that arises from neuroendocrine cells in the intrahepatic biliary epithelium.

When a primary NEN is detected in the liver, a diagnosis of a primary extrahepatic tumor must be excluded; indeed, more than 80% of hepatic NENs are secondary. SPECT/CT with octreotide and Ga68 DOTA-somatostatin analogs PET/TC are useful for detecting primary NEN. NENs are classified into well-differentiated neuroendocrine tumors (NETs), including three grades (G1, G2, and G3), and poorly differentiated neuroendocrine carcinomas (NECs) according to the 2019 WHO classification system. On CT and MR imaging, primary NET shows typically enhancement during the arterial phase, mimicking HCC or hypervascular metastases (Fig. 12), while wash-out is present on delayed phases in 48% of cases [6]. Furthermore, a capsule may be present on late dynamic phases. By contrast, it may resemble ICC because of delayed enhancement in 26% of cases related to the fibrosis within the lesion [6]. The presence of multiple lesions with internal necrosis or hemorrhage is more commonly related to grade 3 primary NET, while grade 1 tumor usually appears as a well-circumscribed, solitary, solid nodule with arterial enhancement. Large mass often exhibits intralesional cystic areas because of necrotic or hemorrhagic changes. Calcifications with a coarse pattern are usually rare but have been described in some cases as central or peripheral elements (Fig. 12) [25]. Chromogranin A and synaptophysin are the typical markers expressed in primary NET cells. Hepatic NET has a better prognosis than HCC, except for the presence of local invasion, metastases, and carcinoid syndrome. Since there be overlap of imaging features between primary NET and HCC, and metastases or

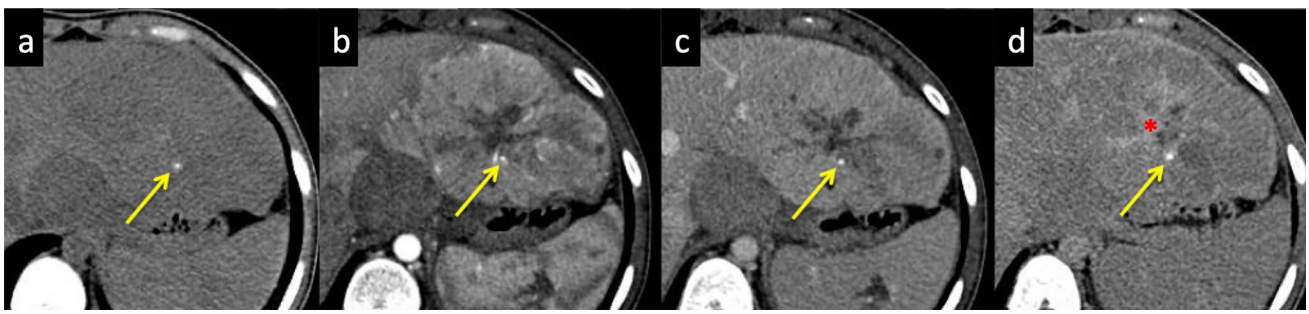

Fig. 11 Fibrolamellar HCC. Unenhanced (**a**) and dynamic contrast-enhanced (**b–d**) CT images exhibit a large lobulated hypervascular hepatic lesion (**b**), without wash-out and with a central stellate scar showing a punctate calcification (arrows) and delayed enhancement (red asterisk) due to its fibrotic component

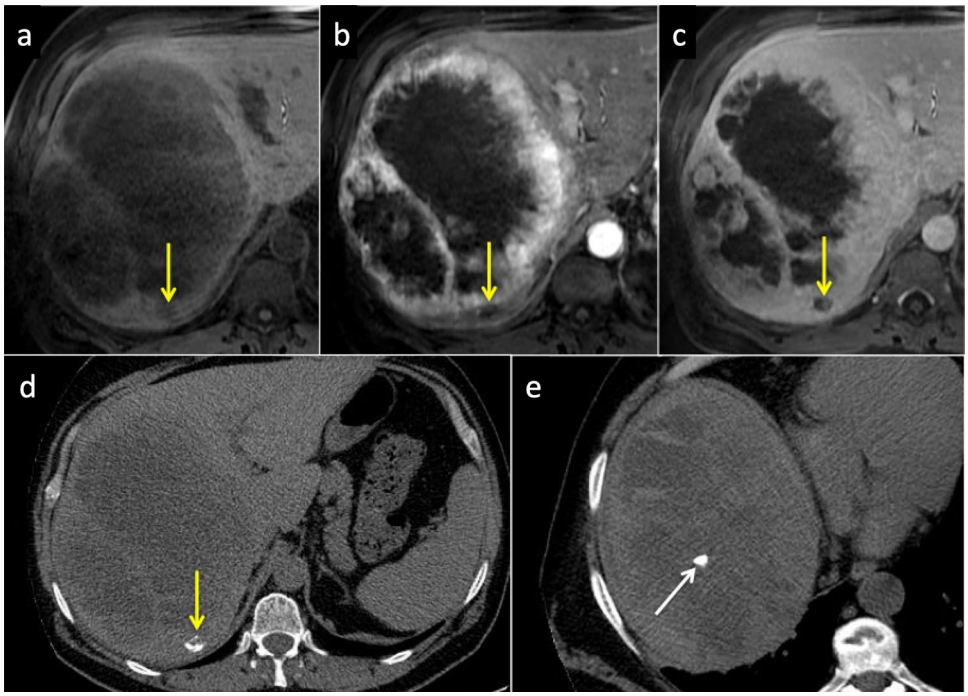

Fig. 12 Neuroendocrine tumor (NET). Axial MR imaging shows a large hepatic mass inhomogeneously hypointense on T1-weighted sequence (**a**), with a mainly peripheral enhancement on arterial (**b**) and portal venous (**c**) phases, a wide area of internal necrosis, and a probable peripheral calcification (yellow arrows). Axial CT images (**d**, **e**) confirm the peripheral calcification (yellow arrow), showing another one in the central part of the mass (white arrow)

ICC, biopsy or surgical resection is often necessary to make the diagnosis.

Calcifications in hypovascular lesions

Hepatoblastoma

Hepatoblastoma is the most common malignancy of the liver in children, usually diagnosed before 5 years of age. Other conditions that may be associated with hepatoblastoma include Gardner syndrome, Beckwith–Wiedemann syndrome, and familial adenomatous polyposis. Hepatoblastoma is classified into epithelial type (56–67%) and mixed epithelial and mesenchymal type (33–44%); furthermore, the fetal subtype has a better prognosis than the small-cell undifferentiated subtype.

This tumor presents as a large, multilobulated, and solitary mass in 80% of cases, associated with alpha fetoprotein elevation in up to 90% of patients [6].

On unenhanced CT, hepatoblastoma is hypodense to the liver parenchyma. Calcifications are observed in 20–50% of lesions (Fig. 13) and are more common in the mixed form [6]. These calcifications are often amorphous and coarse but may be also punctate, speckled, or curvilinear. On contrast-enhanced CT images, hepatoblastoma shows heterogeneous enhancement (more evident in the mixed form) to a lesser degree than the surrounding liver parenchyma in both arterial and portal venous/delayed phases [6]. However, areas of subtle hypervascularization may be present in the arterial

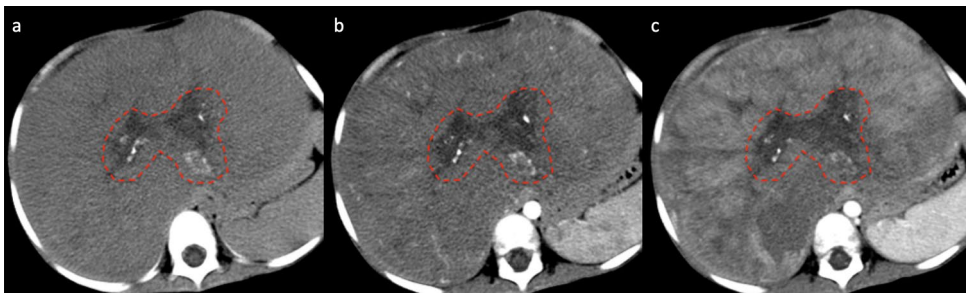

Fig. 13 Hepatoblastoma. Unenhanced (**a**) and dynamic contrast-enhanced CT images on arterial (**b**) and portal venous (**c**) phases show a huge solitary hepatic mass in a child. This tumor shows heterogeneous enhancement with areas of subtle hypervascularization and exhibits multiple, and punctate and amorphous calcifications in its central hypodense portion (red lines), usually related to hemorrhagic areas, necrosis, and fibrotic septa

phase. In addition, hemorrhagic areas, necrosis, and fibrotic septa may be present. Hepatoblastoma shows a tendency toward vascular infiltration, and metastasizes to the lung and abdominal lymph nodes, often at the time of clinical presentation.

Metastases

Hepatic metastases (HMs) are the most common malignancy of the liver, being 18–40 times more common than primary liver tumors [26].

Furthermore, the liver is the second most common site of metastases after lymph nodes. Liver metastatic disease is most commonly related to primary tumors of the gastrointestinal tract, in particular colorectal carcinoma, and to breast and lung cancer.

The imaging findings of HMs depend on the organ of origin and on the vascularity of the lesions. Indeed, they are classified as hypervascular and hypovascular, where the former show arterial enhancement on contrast-enhanced CT imaging, while the latter appear hypodense compared with the surround parenchyma in the same phase.

Hepatic metastases that may develop calcifications are usually hypovascular and related to mucin-producing tumors, in particular from the colorectum and ovary [1, 2]; a rim enhancement or a target appearance in these lesions may even be seen. Calcifications in HMs from colorectal carcinoma before chemotherapy are present in around 11% of cases [27].

Other neoplasms associated with calcified hepatic metastases include stomach and breast carcinoma, pancreatic neuroendocrine tumor, and thyroid medullary carcinoma. Calcified liver metastases from osteosarcoma, chondrosarcoma, leiomyosarcoma, renal carcinoma, lung carcinoma, neuroblastoma, pleural mesothelioma, and melanoma have also been reported.

These calcifications may be central or peripheral in location, and their appearance is variable, from amorphous, stippled, sand-like or granular (Fig. 14) [1].

Importantly, calcifications within liver metastases may be present at the time of diagnosis, but they may also be the result of radiotherapy or systemic chemotherapy. In the latter case, calcifications are usually located in the central part of the lesions. In particular, calcifications from mineralization of necrotic tissue after chemotherapy occur in 5% of patients with HMs from colorectal cancer [28]; although the development of calcifications is considered to be a marker of response to treatment, it does not necessarily correspond to sterilization of the lesion and tumor regrowth is still possible [28, 29].

Sarcoidosis

Sarcoidosis is a systemic disorder characterized by non-necrotizing granulomas. The lung is the most common organ involved, followed by lymph nodes, skin, eyes, liver, heart and the nervous, musculoskeletal, and renal and endocrine systems [30].

Isolated liver involvement without lung disease is rare in sarcoidosis, reported in only 13% of patients [31]. Despite the fact that liver and spleen involvement is reported in 40–60% of cases, symptomatic liver disease occurs in less than 5% of patients. Clinically, patients with liver involvement may be asymptomatic or with symptoms of fever and hepatomegaly.

Hepatomegaly is often associated with adenopathy, splenomegaly, and splenic nodules (more common than hepatic nodules). The hepatic and splenic granulomas are typically innumerable and diffuse, resulting in hepatosplenomegaly on imaging, sometimes with only a diffuse parenchymal heterogeneity [30, 31].

At contrast-enhanced CT imaging, multiple hypodense small lesions scattered throughout the liver are noted in

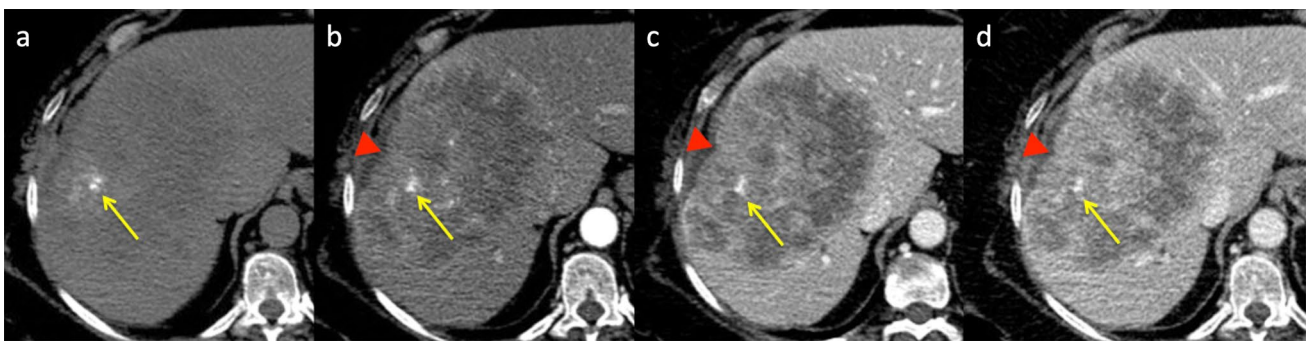

Fig. 14 Metastasis from colorectum adenocarcinoma. Presence of large hepatic mass inhomogeneously hypodense on unenhanced (**a**) and dynamic contrast-enhanced (**b**–**d**) images, showing a central portion of fibrosis associated with stippled, sand-like, and granular calcifications (arrows). Notice the presence of capsular retraction related to the fibrotic component of the lesion (red arrowheads)

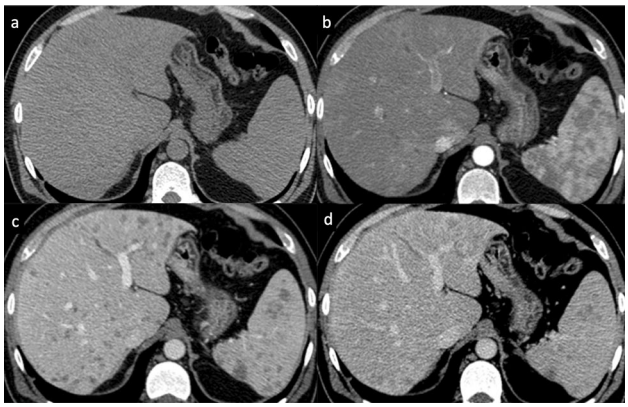

Fig. 15 Sarcoidosis. Unenhanced (**a**) and dynamic contrast-enhanced (**b–d**) CT images in a patient with hepatomegaly and splenomegaly. Notice the presence of multiple hypodense small lesions scattered throughout the liver, better visualized on portal venous phase (**c**), resulting from coalescence of small granulomas (1–2 mm) into macroscopically visible nodules. Calcifications (absent in this case) are uncommon but may be seen in long-standing disease. Splenic hypodense nodules are also present

5–15% of patients, often along the portal tracts, resulting from coalescence of small granulomas (1–2 mm) into macroscopically visible nodules (< 2 cm) (Fig. 15) [30, 31]. These multiple nodules may become isodense to the liver parenchyma on the more delayed post-contrast CT images [31]. The differential diagnosis includes more common diseases such as metastases and lymphoma, or fungal microabscesses and tuberculosis. Calcifications are uncommon in liver sarcoidosis but can be seen in long-standing disease [30]; unfortunately, the pattern of these calcifications is not clearly described in the literature. Portal hypertension, cirrhosis, Budd–Chiari syndrome, and cholestatic disease are hepatic syndromes rarely associated with hepatic sarcoid involvement, secondary to compression of biliary ducts, small intrahepatic portal vein branches, and hepatic veins by granulomatous inflammation [31].

Calcifications in lesions with target appearance

Epithelioid hemangioendothelioma

Hepatic epithelioid hemangioendothelioma (EHE) is a rare tumor of vascular origin with an intermediate malignant potential. It occurs with an incidence of 1:100,000, with a peak incidence between 30 and 50 years of age, and more frequently in females.

EHE typically presents as a solitary lesion or multiple nodules; the multifocal nodular pattern is more common (85% of EHE) than solitary lesion, and the latter can evolve into the multifocal pattern during the follow-up period [6].

The lesions are mainly located peripherally, with enlargement and coalescence in advanced stages. On unenhanced CT, these lesions are hypodense and coarse, and dystrophic calcifications have been reported in up to 20% of cases (Fig. 16) [2, 6], often with a central location. On dynamic contrast-enhanced CT images, EHE shows a target-like appearance (2 or 3 layers) in 67.6% of patients, with a central hypoenhancing area [6, 32]. The 3-layer target appearance reflects the tissue growth pattern of the tumor, with a central sclerotic-fibrous area, a peripheral region of vascularized cellular proliferation and a narrow outer avascular rim caused by tumor infiltration and occlusion of hepatic sinusoids and small vessels [6]. Another enhancement pattern described in EHE is characterized by rim enhancement during the arterial phase, with progressive filling during the delayed phases because of the internal fibrotic area. Because of its peripheral location and its central fibrotic component, the hepatic capsular retraction is considered a typical finding of EHE, reported in 45.4 to 83.3% of tumors [6]. The "lollipop sign" has been described in association with EHE, in

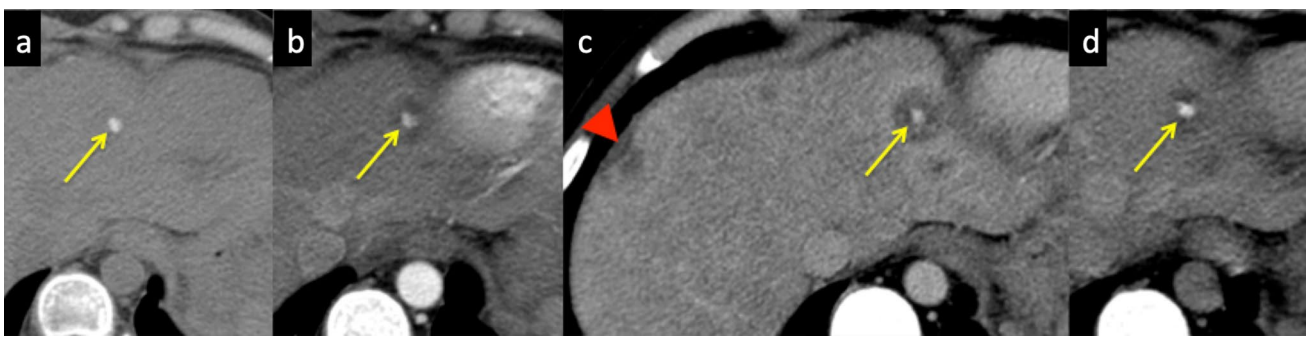

Fig. 16 Epithelioid hemangioendothelioma. Unenhanced (**a**) and dynamic contrast-enhanced (**b–d**) CT images show a round lesion with a target appearance and a central small calcification (arrows). On portal venous phase (**c**), notice the presence of multiple peripheral lesions and capsular retraction (arrowhead)

which the candy in the lollipop represents the lesion and the stick of the lollipop refers to the adjacent occluded portal or hepatic veins [6, 32]. Furthermore, EHE can metastasize to lymph nodes, peritoneum, lung, and bone. The main differential diagnosis includes hepatic metastases from adenocarcinoma. A known primary malignancy and the absence of capsular retraction help in the diagnosis.

Brucellosis

Brucellosis is one of the most common zoonosis worldwide. Though hepatosplenomegaly and mild elevation of liver enzyme levels are the typical signs of this disease, abscess formation in the liver (brucelloma) and spleen is possible and well described in the literature [33]. A liver brucelloma appears as a pseudotumoral mass, heterogeneously hypodense on contrast-enhanced CT imaging; in addition, a peripheral enhancing rim may even be seen. As typical finding, a central solitary calcification is often present, surrounded or not by a fluid collection, and should bring to mind a diagnosis of brucellosis (Fig. 17) [33].

Pyogenic abscess

Pyogenic hepatic abscesses are pus-filled masses in the liver that can develop from cholangitis or an intra-abdominal infection through the portal vein. They are usually polymicrobial, where the most common bacterial agents include E. coli, Klebsiella, Staphylococcus, Streptococcus, and anaerobic organisms. The appearance of liver abscesses on CT is variable: (1) hypoattenuating lesions with peripheral enhancement; (2) lesion with the "double target sign," which consists of a central fluid low attenuation area, surrounded by an enhancing inner rim (abscess membrane) and a low attenuation outer ring representing parenchymal edema; (3) lesion with the "cluster sign," which consists of a multiloculated appearance resulting from aggregation of multiple small low attenuation lesions to form a solitary larger abscess [34]. Pyogenic hepatic abscesses may contain gas in up to 20% of cases, in the form of bubbles or air-fluid levels [34]. Furthermore, a perfusion abnormality (THAD) may be seen surrounding the lesion [34]. Central or peripheral calcifications may be present in chronic abscesses or in some residual lesions (Fig. 18).

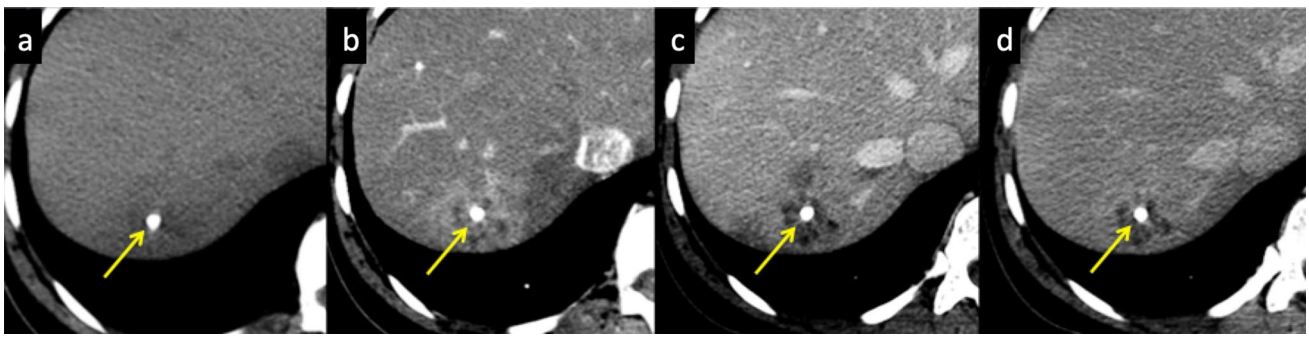

Fig. 17 Brucellosis. Unenhanced (**a**) and dynamic contrast-enhanced (**b**–**d**) CT images show a subcapsular lobulated lesion, characterized by inhomogeneous enhancement, reactive ring enhancement on arterial phase (**b**), hypodense surrounding parenchymal edema, (**c**) and a typical central calcification (arrows)

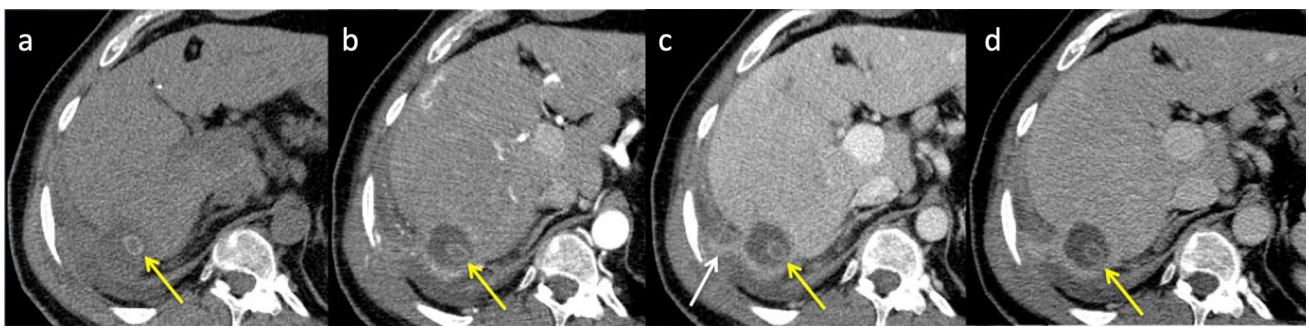

Fig. 18 Pyogenic abscess. Unenhanced (**a**) and dynamic contrast-enhanced (**b**–**d**) CT images show a subcapsular exophytic lesion, with rim enhancement and a wide internal necrosis associated with a solitary nodular calcification (arrows). Notice the fistulization to the diaphragm and to the abdominal wall (white arrow), and pleural effusion

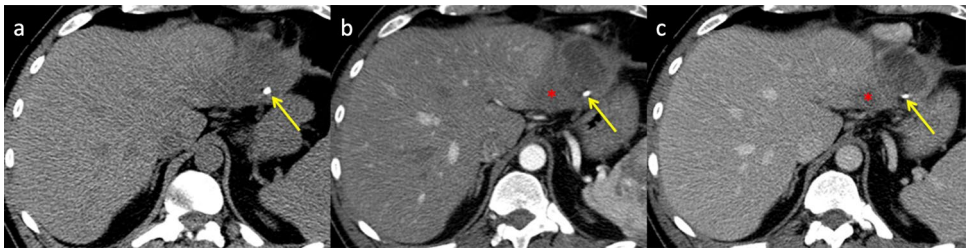

Fig. 19 Amoebic abscess. Unenhanced (**a**) and dynamic contrast-enhanced CT images on arterial (**b**) and portal venous (**c**) phases show a subcapsular lesion on the left hepatic lobe, with a complex fluid attenuation in the central part and a capsule with rim enhancement. Notice the presence of a small calcification in the periphery of the lesion (arrows) and a hypodense area of edema in the surrounding parenchyma (asterisk)

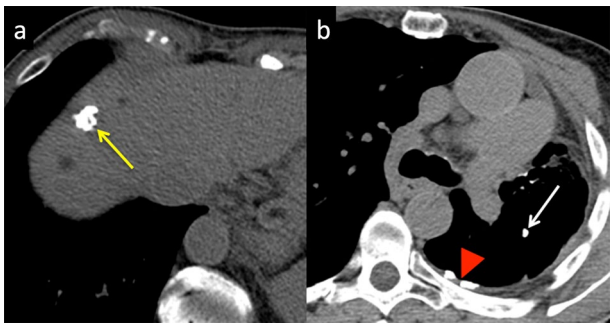

Fig. 20 Tuberculosis. Unenhanced CT image of the liver (**a**) shows a small (< 2 cm) and solitary granuloma with amorphous calcification typically involving the entire lesion (yellow arrow). In the same patient, unenhanced CT image of the left lung (**b**) shows the presence of a small calcified granulomas (white arrow) and calcified pleural plaques (red arrowhead), as signs of tubercular disease

Amoebic abscess

Amoebic hepatic abscess is a form of hepatic abscess resulting from Entamoeba histolytica infection. On CT, it is usually unilocular and located near the hepatic capsule, with a complex fluid attenuation in the central part of the lesion and a capsule with rim enhancement or the "double target sign," mimicking the pyogenic abscess [34]. Though often unilocular, internal septa may be present in 30% of amoebic abscess [34]. A peripheral zone of edema in the surrounding parenchyma may be present and after healing the periphery of the amoebic abscess may calcify (Fig. 19).

Isolated calcifications

The most common causes of isolated calcifications in the liver are infections, in particular resulting in granuloma formation. Tuberculosis and histoplasmosis are the most common infections associated with granuloma formation. These granulomas are small (< 2 cm), solitary or multiple, and with calcification typically involving the entire lesion in clinically occult or healed lesions (Fig. 20) [1, 2]. The presence of calcified granulomas in the lungs and spleen helps in the diagnosis of granulomatous disease (Fig. 20) [1, 2].

Regarding hepatic tuberculosis, indeed, the miliary type is the most common pattern usually associated with disseminated disease and showing numerous, small (< 2 cm), and hypodense nodules scattered throughout the liver. In contrast, isolated hepatic tuberculosis is rarely described but can show different imaging patterns [2] and confounded with neoplastic lesions: the serohepatic type (multiple confluent subcapsular hypodense lesions associated with nodular or irregular fusiform calcifications); the cystic type (cystic lesions without enhancement); the nodular type (hypodense lesion > 2 cm with irregular, peripheral, and curvilinear calcifications or a central calcification); the mixed type (CT findings of both serohepatic and cystic and nodular types); tubercular cholangitis (biliary dilatation with ductal wall calcifications).

Schistosomiasis is one of most frequent parasitic infection. It is caused by an infection of trematodes, Schistosoma (in particular *Schistosoma japonicum*), leading to periportal fibrosis, which can result in presinusoidal portal hypertension, with splenomegaly and gastroesophageal varices [1, 35]. Indeed, the deposition of eggs in the small portal venules causes a granulomatous inflammatory response, followed by fibrosis [1, 35]. Imaging findings of the liver are multiple peripheral subcapsular and periportal wedge-shaped hypoattenuating regions associated with capsular retraction [35]. Capsular and peripheral septal calcifications may be present and when extensive have been described as “turtle back” pattern [1]. Egg-shell urothelial calcifications may be noted throughout the ureters and the urinary bladder, in particular in S. haematobium.

Conclusion

Calcifications may be seen in a vast spectrum of liver focal lesions. Therefore, radiologists should be aware of the most common causes of liver calcifications. Though their

morphologic appearances alone do not allow a specific diagnosis, the association with other imaging findings of the calcified lesions, clinical presentation, and laboratory tests may indicate the correct diagnosis or narrow the differential diagnosis.

Funding The authors declare no financial support.

Compliance with ethical standards

Conflict of interest The authors declare no conflict of interest.

Informed consent Our Institutional Research Review Board reviewed and approved this article, with waiver of the informed consent; a written informed consent to the MR procedures was obtained after a full explanation of the purpose and nature of the procedure.

References

1. Stoupis, C., et al., The Rocky liver: radiologic-pathologic correlation of calcified hepatic masses. Radiographics, 1998. 18(3): p. 675–85; quiz 726.
2. Patnana, M., et al., Liver Calcifications and Calcified Liver Masses: Pattern Recognition Approach on CT. AJR Am J Roentgenol, 2018. 211(1): p. 76–86.
3. Borhani, A.A., A. Wiant, and M.T. Heller, Cystic hepatic lesions: a review and an algorithmic approach. AJR Am J Roentgenol, 2014. 203(6): p. 1192–204.
4. Mortele, K.J. and H.E. Peters, Multimodality imaging of common and uncommon cystic focal liver lesions. Semin Ultrasound CT MR, 2009. 30(5): p. 368–86.
5. Qian, L.J., et al., Spectrum of multilocular cystic hepatic lesions: CT and MR imaging findings with pathologic correlation. Radiographics, 2013. 33(5): p. 1419–33.
6. Mamone, G., et al., Imaging of primary malignant tumors in non-cirrhotic liver. Diagn Interv Imaging, 2020. 101(9): p. 519–535.
7. Choi, B.I., et al., Biliary cystadenoma and cystadenocarcinoma: CT and sonographic findings. Radiology, 1989. 171(1): p. 57–61.
8. Korobkin, M., et al., Biliary cystadenoma and cystadenocarcinoma: CT and sonographic findings. AJR Am J Roentgenol, 1989. 153(3): p. 507–11.
9. Marrone, G., et al., Multidisciplinary imaging of liver hydatidosis. World J Gastroenterol, 2012. 18(13): p. 1438–47.
10. Polat, P., et al., Hydatid disease from head to toe. Radiographics, 2003. 23(2): p. 475–94; quiz 536–7.
11. Mamone, G., et al., Magnetic resonance imaging of fibropolycystic liver disease: the spectrum of ductal plate malformations. Abdom Radiol (NY), 2019. 44(6): p. 2156–2171.
12. Mamone, G., et al., Imaging of hepatic hemangioma: from A to Z. Abdom Radiol (NY), 2020. 45(3): p. 672–691.
13. Paley, M.R. and P.R. Ros, Hepatic calcification. Radiol Clin North Am, 1998. 36(2): p. 391–8.
14. Mamone, G., et al., Intrahepatic mass-forming cholangiocarcinoma: enhancement pattern on Gd-BOPTA-MRI with emphasis of hepatobiliary phase. Abdom Imaging, 2015. 40(7): p. 2313–22.
15. Nault, J.C., et al., Molecular Classification of Hepatocellular Adenoma Associates With Risk Factors, Bleeding, and Malignant Transformation. Gastroenterology, 2017. 152(4): p. 880–894 e6.
16. Zulfiqar, M., et al., Hepatocellular adenomas: Understanding the pathomolecular lexicon, MRI features, terminology, and pitfalls to inform a standardized approach. J Magn Reson Imaging, 2019.
17. Nault, J.C., et al., Molecular classification of hepatocellular adenoma in clinical practice. J Hepatol, 2017. 67(5): p. 1074–1083.
18. Grazioli, L., et al., Hepatic adenomas: imaging and pathologic findings. Radiographics, 2001. 21(4): p. 877–92; discussion 892–4.
19. Ichikawa, T., et al., Hepatocellular adenoma: multiphasic CT and histopathologic findings in 25 patients. Radiology, 2000. 214(3): p. 861–8.
20. Chernyak, V., et al., Liver Imaging Reporting and Data System (LI-RADS) Version 2018: Imaging of Hepatocellular Carcinoma in At-Risk Patients. Radiology, 2018. 289(3): p. 816–830.
21. Freeny, P.C., R.L. Baron, and S.A. Teefey, Hepatocellular carcinoma: reduced frequency of typical findings with dynamic contrast-enhanced CT in a non-Asian population. Radiology, 1992. 182(1): p. 143–8.
22. Stevens, W.R., et al., CT findings in hepatocellular carcinoma: correlation of tumor characteristics with causative factors, tumor size, and histologic tumor grade. Radiology, 1994. 191(2): p. 531–7.
23. Ganeshan, D., et al., Fibrolamellar hepatocellular carcinoma: multiphasic CT features of the primary tumor on pre-therapy CT and pattern of distant metastases. Abdom Radiol (NY), 2018. 43(12): p. 3340–3348.
24. Ichikawa, T., et al., Fibrolamellar hepatocellular carcinoma: imaging and pathologic findings in 31 recent cases. Radiology, 1999. 213(2): p. 352–61.
25. Meng, X.F., et al., Primary hepatic neuroendocrine tumor case with a preoperative course of 26 years: A case report and literature review. World J Gastroenterol, 2018. 24(24): p. 2640–2646.
26. Imam, K. and D.A. Bluemke, MR imaging in the evaluation of hepatic metastases. Magn Reson Imaging Clin N Am, 2000. 8(4): p. 741–56.
27. Hale, H.L., et al., CT of calcified liver metastases in colorectal carcinoma. Clin Radiol, 1998. 53(10): p. 735–41.
28. Zhou, Y., et al., Tumor calcification as a prognostic factor in cetuximab plus chemotherapy-treated patients with metastatic colorectal cancer. Anticancer Drugs, 2019. 30(2): p. 195–200.
29. Goyer, P., et al., Complete calcification of colorectal liver metastases on imaging after chemotherapy does not indicate sterilization of disease. J Visc Surg, 2012. 149(4): p. e271–4.
30. Vagal, A.S., R. Shipley, and C.A. Meyer, Radiological manifestations of sarcoidosis. Clin Dermatol, 2007. 25(3): p. 312–25.
31. Guidry, C., et al., Imaging of Sarcoidosis: A Contemporary Review. Radiol Clin North Am, 2016. 54(3): p. 519–34.
32. Mamone, G. and R. Miraglia, The "Target sign" and the "Lollipop sign" in hepatic epithelioid hemangioendothelioma. Abdom Radiol (NY), 2019. 44(4): p. 1617–1620.
33. Sisteron, O., et al., Hepatic abscess caused by Brucella US, CT and MRI findings: case report and review of the literature. Clin Imaging, 2002. 26(6): p. 414–7.
34. Bachler, P., et al., Multimodality Imaging of Liver Infections: Differential Diagnosis and Potential Pitfalls. Radiographics, 2016. 36(4): p. 1001–23.
35. Mamone, G., et al., Hepatic morphology abnormalities: beyond cirrhosis. Abdom Radiol (NY), 2018. 43(7): p. 1612–1626.